PCCP

Accepted Manuscript

ROYAL SOCIETY OF CHEMISTRY

www.rsc.org/pccp

Control of incorporation of pyridinic, pyrrolic, graphitic, and molecular nitrogen in multi-wall carbon nanotubes *via* the N/C ratio in aerosol assisted chemical vapor deposition

L.G. Bulusheva[a,b,1], A.V. Okotrub[a,b], Yu.V. Fedoseeva[a,b], A.G. Kurenya[a], I.P. Asanov[a,b], O.Y. Vilkov[c], A.A. Koós[d], and N. Grobert[d]

[a]Nikolaev Institute of Inorganic Chemistry, SB RAS, 630090 Novosibirsk, Russia

[b]Novosibirsk State University, 630090 Novosibirsk, Russia

[c]St. Petersburg State University, 198504 St. Petersburg, Russia

[d]Department of Materials, University of Oxford, Oxford OX1 3PH, UK[2]

Abstract

Nitrogen-containing multi-wall carbon nanotubes (N–MWCNTs) were synthesized using aerosol assisted chemical vapor deposition (CVD) techniques in conjunction with benzylamine:ferrocene or acetonitrile:ferrocene mixtures. Different amounts of toluene were added to these mixtures in order to change the N/C ratio of the feedstock. X-ray photoelectron and near-edge X-ray absorption fine structure spectroscopy detected pyridinic, pyrrolic, graphitic, and molecular nitrogen forms in the N–MWCNT samples. Analysis of the spectral data indicated that whilst the nature of nitrogen-containing precursor has little effect on the concentrations of the different forms of nitrogen in N–MWCNTs, the N/C ratio in the feedstock appeared to be the determining factor. When the N/C ratio was lower than *ca.* 0.01, all four forms existed in equal concentrations, for N/C ratios above 0.01, graphitic and molecular nitrogen were dominant. Furthermore, higher concentrations of pyridinic nitrogen in the outer shells and N_2 molecules in the core of the as-produced N–MWCNTs suggest that the precursors were decomposed to individual atoms, which interacted with the catalyst surface to form CN and NH species or in fact diffused through the bulk of catalyst particle. This finding is important for understanding the growth mechanism of CNTs and controlling the spatial distribution of foreign elements in nanotube body using the CVD process.

[1]Corresponding author, e-mail: bul@niic.nsc.ru

[2]Present address: Institute for Technical Physics and Materials Science, Konkoly-Thege ut. 29-33, 1121 Budapest, Hungary

1. Introduction

Incorporation of nitrogen atoms in the walls of carbon nanotubes (CNTs) is an attractive way for the tuning their electronic and chemical properties.[1–3] Particularly, as compared to the pure counterparts, nitrogen-containing CNTs (N–CNTs) exhibit better performance as cold electron emitters,[4–6] supports for catalyst nanoparticles,[7–9] electrodes in electrochemical capacitors[10, 11] and Li-ion batteries.[12, 13] Catalytic chemical vapor deposition (CCVD) techniques are well established and widely applied for the generation of N–CNTs. It was shown that the concentration and the type of nitrogen depend on the synthesis temperature, gas flow rate, and nature of the catalyst as well as the type of nitrogen precursor.[14–17] The most common forms of imbedded nitrogen discussed in the literature are graphitic, pyridinic and pyrrolic nitrogen.[1, 18–20] Graphitic nitrogen refers to a nitrogen atom with three carbon neighbors in a hexagonal lattice, if the nitrogen is two-fold coordinated similar to that is found in pyridine, it is called pyridinic, and three-fold coordinated nitrogen in a region of defective non-aromatic lattice is associated with pyrrolic nitrogen. While the majority of reports argue that, due to their different stabilities, the concentration of these different types of nitrogen atoms in N–CNTs is largely controlled by the synthesis temperature[21, 22] some accounts also consider the nature of the precursor to be a crucial factor. For instance, when acetonitrile was mixed with short-chain alcohols, pyridinic nitrogen was not observed in N–CNTs.[23] With increasing melamine concentration in the feedstock material, an increase in the ratio of pyridinic to graphitic nitrogen was observed and attributed to the presence of the CN bonds in the precursor contributing to the pyridinic nitrogen formation.[24] Jian *et al.* conducted a study using different nitrogen-containing precursors with the aim to control the type of nitrogen atoms present in the N–CNTs whereby the precursors contained nitrogen atoms in an aromatic ring and/or in an amine group.[25] Whilst the investigation revealed a general increase of nitrogen in the N–CNT product with increasing N/C ratios in the initial precursor, the variation of the forms of the imbedded nitrogen atoms was not discussed and most likely because no dependence could be identified. Comparison of the amines and amides

precursors for the N–CNT growth showed that the N/C ratio in the feedstock material has a more noticeable effect on the morphology and nanotube yield, than the actual nature of the nitrogen source.[26]

The mechanism of CCVD growth of CNTs is not yet fully understood[27] and the question how the type of C–N bonding in the precursor may influence the forms of the incorporated nitrogen remains open. For nanotubes to form, the first step necessary in the synthesis process is the decomposition of a solid, liquid or gaseous carbon-containing precursor, on a catalytic surface which can be a metal thin film or metal catalyst particles. However, the products of the cracking of the nitrogen-containing precursor molecules are usually unknown.[28] It could be atoms, dimers, or stable fragments such as, for example, phenyl. The second step in the growth process includes the diffusion of the cracking products through the bulk of a catalyst, in the subsurface layers, or on the surface of the catalyst particle followed by the extrusion of the carbon to form a nanotube.[29] Studies using density functional theory (DFT) revealed that atomic carbon and nitrogen possess quite small energy barriers with regards to their mobility on an iron cluster, and tend to interact readily, producing C_2 and CN units.[30] Molecular dynamic simulation confirmed that these units move faster on iron nanoparticle surfaces than individual atoms do.[31] Therefore, the direct dependence between pre-existing CN bonds in the precursor and the predominant form of nitrogen in the N–CNTs can be expected only if the precursor dissociates incompletely and the obtained N-containing species diffuse on the surface of a catalyst particle.

Here, we study the presence of the different forms of nitrogen in multi-wall CNTs (N–MWCNTs) using precursors containing CN and NH_2 bonds, namely, acetonitrile (CH_3CN) and benzylamine ($C_6H_5CH_2NH_2$) in conjunction with aerosol assisted CCVD, where ferrocene was used as a catalyst source. Acetonitrile contains triple CN bond, which could be the source of the pyridinic nitrogen, while NH_2 species in benzylamine may contribute to the graphitic or pyrrolic nitrogen atoms. X-ray photoelectron spectroscopy (XPS) and near-edge X-ray absorption fine structure (NEXAFS) spectroscopy were used to identify the concentration and electronic state of

nitrogen in the N–MWCNTs. The former spectroscopy is surface-sensitive and the latter one probes the bulk of a nanotube. Combination of these methods allows detecting a change in the distribution of nitrogen forms from the outer layer to the nanotube core.

2. Experimental

Details of the aerosol assisted CVD setup used for the synthesis of N–MWCNTs studied here can be found elsewhere. N–MWCNTs were produced with solutions of 5 wt% ferrocene [$Fe(C_5H_5)_2$] in benzylamine[32] and acetonitrile.[33] The N/C ratio is 1:2 in acetonitrile and 1:7 in benzylamine. In order to change this ratio, a certain portion (5:95, 50:50, and 100:0) of toluene $C_6H_5CH_3$ was added to the reaction mixture. When the horizontal tubular reactor reached 800°C, the precursor solutions were introduced with an Ar flow rate of 0.14 ml/min at atmospheric pressure over a period of 30 min. The synthesis temperature and gas flow rate were kept constant throughout the experiment in order to minimize any possible the influence of these parameters on the incorporation of the nitrogen.

The structure of the as-produced N–MWCNTs samples was examined by transmission electron microscopy (TEM, Jeol 2010). IR-absorption spectra were recorded using a Fourier transform spectrometer FTS–2000 by pressing the sample with KBr.

XPS and NEXAFS spectra were recorded at the Berliner Elektronenspeicherring für Synchrotronstrahlung (BESSY) using radiation from the Russian-German beamline. XPS spectra were measured at energy of monochromatized synchrotron radiation equal to 800 eV. NEXAFS spectra near the N K-edge were acquired in the total-electron yield (TEY) mode with the monochromatization of the incident radiation of ~0.17 eV. The spectra were normalized to the primary photon current from a gold-covered grid recorded simultaneously. To study the change in electronic state of nitrogen in the nanotube depth, the XPS spectra were recorded on a Phoibos 150 Specs spectrometer using nonmonochromatic Mg K_α (1253.6 eV) excitation. The binding energies were calibrated relative to the C 1s peak at 284.5 eV.

3. Results

TEM analysis confirmed the presence of multi-wall nanotubes in all samples. A change in the nanotube structure was also observed depending on the N/C ratio in the hydrocarbon feedstock and an example of such change is presented in Figure 1 showing N–MWCNTs grown from acetonitrile:toluene mixtures of (a) 5:95, (b) 50:50, and (c) 100:0. At the lowest N/C ratio of 1/135 for a precursor ratio of 5:95, the nanotubes exhibit relatively straight and thick walls of ~12 nm in average (Fig. 1a). Higher nitrogen concentrations cause a reduction of the number and corrugation of the carbon layers while the diameter of the inner core increases (Fig. 1b, c). Similar structural variation was observed when N–MWCNTs were grown from mixtures of benzylamine/toluene,[32, 34] melamine/ethylene,[24] or ammonia/acetylene.[35]

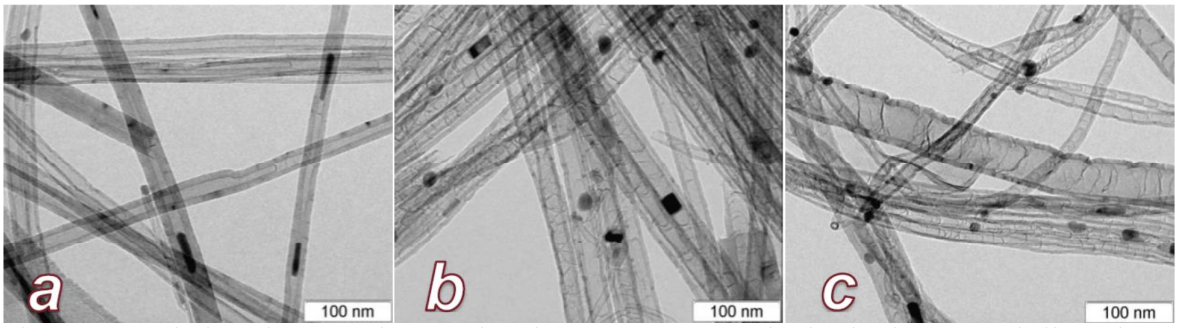

Fig. 1 Transmission electron micrographs of N–MWCNTs synthesized using acetonitrile and toluene mixed in ratios of 5:95 (a), 50:50 (b), and 100:0 (c).

The nitrogen content in the N–MWCNTs was determined from the ratio of the areas under the C 1s and N 1s peaks taking into consideration the photoionization cross-sections for elements at the given photon energy. The values derived from the survey spectra measured at 800 eV are summarised in Table 1. There is a tendency of enrichment of nitrogen in the nanotubes with higher N/C ratios in the feedstock. N 1s spectra (Fig. 2) revealed the nature of the incorporated nitrogen atoms. Based on the N K-edge NEXAFS spectra, which we will be addressed later, three components located at 398.5, 399.9, and 401.1 eV were separated in the XPS spectra. With increasing binding energies, the components correspond to pyridinic, pyrrolic, and graphitic nitrogen and we found that the relation between the N/C ratio in feedstock and the

concentration of the respective nitrogen forms incorporated in the N–MWCNTs is ambiguous (Table 1). Our findings show that in both samples produced with *ca.* 5 % of benzylamine or acetonitrile the different nitrogen forms were present in equal concentrations in the N–MWCNTs. However, when the portion of a nitrogen-containing hydrocarbon increases, the contribution of pyrrolic nitrogen in the N 1s spectrum progressively diminishes. The components corresponding to the graphitic nitrogen and pyridinic nitrogen have almost equal intensities in the spectra of all investigated N–MWCNTs except those synthesized from a mixture of acetonitrile:toluene of 50:50 and from benzylamine solely, where the graphitic nitrogen noticeably prevails.

Table 1 The correlation between the N/C ratio in the hydrocarbon precursors and the total nitrogen content (N_{tot}) and the ratio of pyridinic, pyrrolic, and graphitic nitrogen in the as-produced N–MWCNTs using benzylamine or acetonitrile. The concentration of nitrogen was determined using survey X-ray photoelectron spectra measured at 800 eV.

N/C	1/140	1/135	1/14	1/9	1/7	1/2
N-source	$C_7H_7NH_2$	CH_3CN	$C_7H_7NH_2$	CH_3CN	$C_7H_7NH_2$	CH_3CN
N_{tot} (at%)	0.1	0.8	0.4	1.2	1.0	3.0
N_{pyrid}: N_{pyrr}: N_{gr}	1:1:1	1:1:1	2:1:2	1.3:1:2.4	3.4:1:8	4:1:4

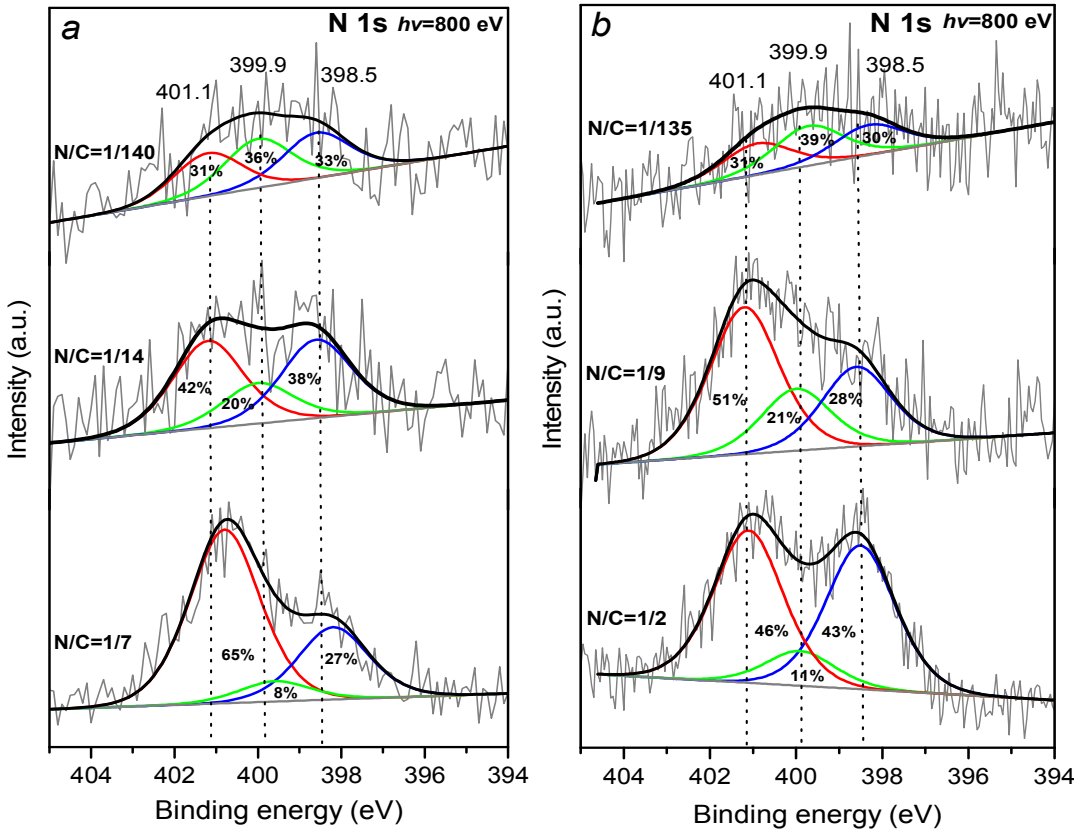

Fig. 2 XPS N 1s spectra of N–MWCNTs synthesized from (a) benzylamine (N/C=1/140) or benzylamine mixed with 50% of toluene (N/C=1/14) and 95% of toluene (N/C=1/7) and (b) acetonitrile (N/C=1/135) or acetonitrile mixed with 50% of toluene (N/C=1/9) and 95% of toluene (N/C=1/2). The spectra were collected with an excitation energy of 800 eV.

At excitation energy of 800 eV, the inelastic mean free path of photoelectrons from the N 1s level is estimated to be ~1.8 nm.[36] Hence, the proportions of different nitrogen forms determined from the XPS spectra fitting (Table 1) correspond to about 5 outer layers of the N–MWCNTs. Increase of the photon energy to 1253.6 eV allows registering the photoelectrons from about 7–8 surface layers. The N 1s spectrum measured at this energy for the sample synthesized from benzylamine is shown in Fig. 3. In this particular case, a Doniach-Sunjic high-energy tail with an asymmetry factor[37] of 0.04 was added to a Gausssian/Lorentzian product function to describe the main spectral component at ~401.1 eV. The asymmetric tail may be related with a satellite arisen from the energy loss of electrons associated to the occupied-unoccupied states contributed by nitrogen.[38] The N 1s spectrum has a reduced relative area of the component caused by pyridinic nitrogen atoms when compared to the spectrum recorded at 800 eV (Fig. 2a). This implies that pyridinic nitrogen prefers to be in the surface layers. In addition, the spectrum exhibits a component at ~405.1 eV assigned to N_2 molecules.[39] High-resolution TEM images revealed that the number of layers in the N–MWCNTs in not less than seven. The absence of the signal from the molecular nitrogen in the spectrum recorded at the photon energy of 800 eV and its appearance when the energy was increased to 1253.6 eV indicates that the N_2 molecules are located between the inner layers or in the nanotube cavity. Scanning transmission X-ray microscopy studies of an individual nitrogen-containing nanotube by Zhou et al. revealed the presence of pyridinic and graphitic nitrogen atoms in surface layers and N_2 molecules inside the core of the nanotube.[40] Our studies of bulk quantities of N-MWCNTs complement these findings.

The average nitrogen content in the sample derived from the XPS data obtained at 1253.6 eV is ~1.2 at%, which is higher than that found in the first five nanotube layers (Table 1). Previously, it was shown that N–MWCNTs synthesized from phthalocyanines also showed

higher nitrogen levels near the surface rather than in the inner core.[41] In our case, increase in the total nitrogen content is accompanied with a raise of the portions of graphitic and molecular nitrogen.

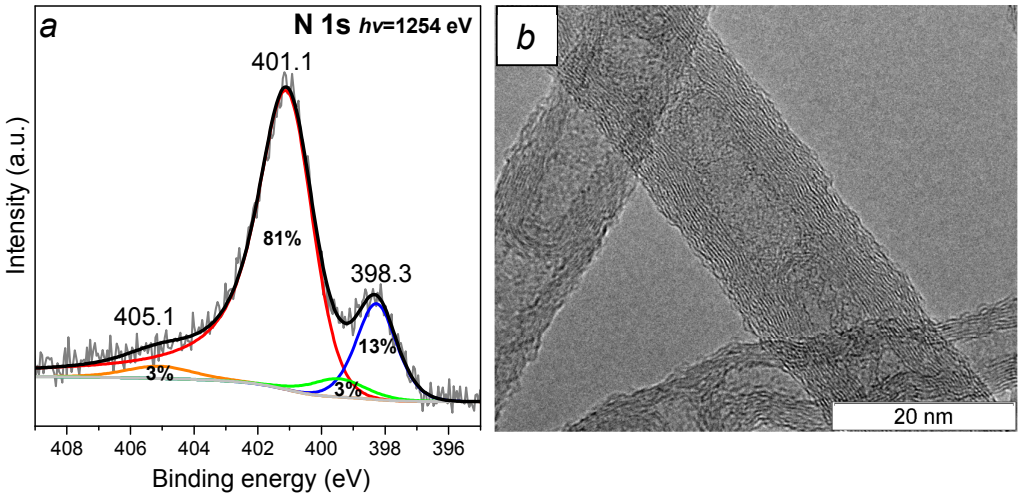

Fig. 3 XPS N 1s spectrum (a) and high-resolution TEM image (b) of N–MWCNTs synthesized from benzylamine. The spectrum was collected with an excitation energy of 1253.6 eV.

NEXAFS spectroscopy in the TEY mode registers the photoelectrons of depths greater than 10 nm from the surface, thus providing compositional information not only of the nanotube walls but also probing the nanotube core. Figure 4 compares the spectra measured near the N K-edge of the synthesized samples. At energies lower than the σ*edge the spectra show a set of resonances and in the following we firstly focus on the most intense peak. The peak splitting corresponds to the vibrational fine structure of N_2 molecules in N–CNTs.[42, 43] The spectrum of the sample produced from acetonitrile solely exhibits the highest relative intensity of the peak (see Fig. 4b). This intensity progressively decreases with lower nitrogen contents in the feedstock (Fig. 4). The ratio of the heights of the N_2 resonance and σ* resonance equals ~0.67 for a N/C ratio of 1/9 (50% of acetonitrile and 50% of toluene) and ~0.82 for the ratio of 1/7 (100% of benzylamine). Interestingly, N_2 molecules are also formed even at very low nitrogen contents in the precursor (1/140 for the mixture of benzylamine and toluene of 5:95). Moreover,

the N K-edge spectra show a broad resonance around 398.6–398.7 eV and a resonance at ~400.0 eV, which can be attributed to the pyridinic and pyrrolic nitrogen in line with the XPS data. The latter π* resonance has the energy close to that of the nitril C≡N groups.[44]

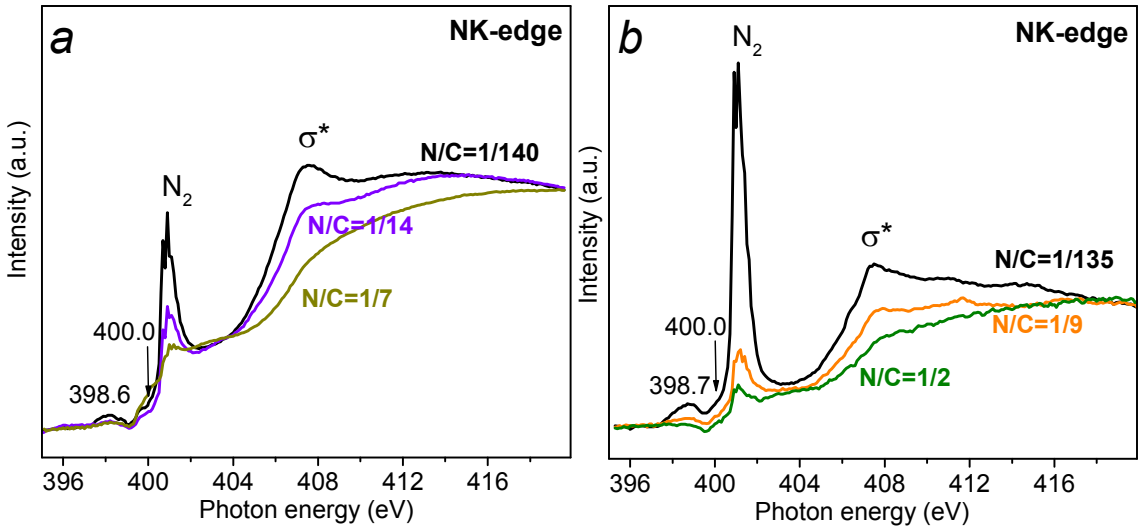

Fig. 4 NEXAFS N K-edge spectra of N–MWCNTs synthesized using (a) benzylamine (N/C=1/140), benzylamine mixed with 50% of toluene (N/C=1/14) or 95% of toluene (N/C=1/7) and (b) acetonitrile (N/C=1/135), acetonitrile mixed with 50% of toluene (N/C=1/9) or 95% of toluene (N/C=1/2).

Although it is difficult imagining how these groups can accommodate between the nanotube layers, we measured IR-spectrum for the sample produced from the acetonitrile and toluene taken in equal proportion, because the N 1s spectrum of this sample showed a high intensity of the center component of the spectrum (Fig. 2b). Vibration of the triple C≡N bond is expected around 2220 cm^{-1},[45] and there the spectrum showed a negligible absorption (Fig. 5). Thus, we suggest that the nitrogen atoms adopts an intermediate state between pyridinic and graphitic nitrogen corresponding to pyrrolic nitrogen atoms. The N–H vibrations around 3200 cm^{-1} are overlapped with the O–H bond vibrations. The resonance related with the 1s→π* transitions within the graphitic nitrogen should appear at ~401.0 eV and in our spectra it is masked by the N_2 resonance. However, this type of nitrogen is responsible for a strong σ* resonance[46] thus increasing relative intensity of the σ* edge when the amount of trapped N_2

molecules is reduced. Overall, the concentration of all forms of nitrogen decreases with the decrease of the N/C ratio in the feedstock used for the synthesis of N–MWCNTs.

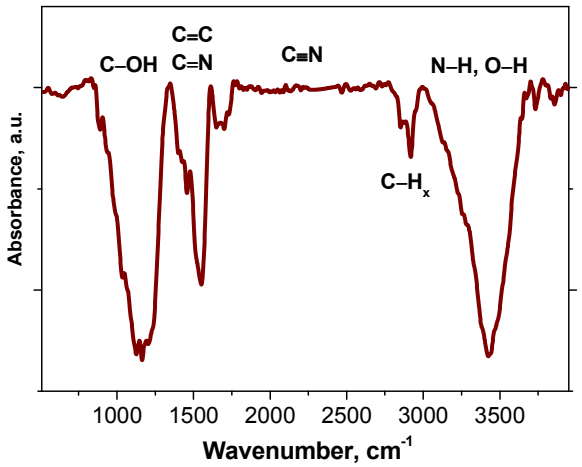

Fig. 5 IR spectrum of N–MWCNTs synthesized from acetonitrile mixed with toluene (50:50).

4. Discussion

XPS and NEXAFS analyses of the N–MWCNT samples synthesized by an aerosol assisted CCVD method revealed graphitic, pyridinic, pyrrolic, and molecular forms of nitrogen. When concentration of nitrogen in precursor was low (one nitrogen atom per hundreds of carbon atoms), there was no marked preference of any form. This is a new result; earlier studies using such low N/C ratio of the reactants have been focused on structural configurations of the N–MWCNTs.[26, 32] Increasing the N/C ratio of up to an order of magnitude suppressed the formation of pyrrolic nitrogen. Independently of the use of benzylamine or acetonitrile as the precursor, the outer layers of the N–MWCNTs synthesized at 800°C contained mainly pyridinic nitrogen while the core stored N_2 gas. Previous studies of double-walled N–CNTs by Kim *et al.* showed a larger fraction of pyridinic nitrogen in the inner walls[47] of the nanotubes. This nitrogen form was suggested to release a strain of the curved graphitic sheets better than graphitic nitrogen. In our case, such strain-releasing effect should be negligible due to the comparatively large diameters of the N–MWCNTs.

Formation of the pyrrolic nitrogen in nanotubes grown from acetonitrile, containing no N–H bonds, evidenced that the precursor was completely decomposed on the surface of catalytic

nanoparticle. The consequent interaction of the nitrogen and hydrogen atoms giving NH species is in accordance with the theoretical considerations of the N–CNT generation.[30, 31] Catalytic cracking of acetonitrile produces more nitrogen atoms as compared to that of benzylamine, and the large fraction of pyridinic nitrogen in the surface layer of nanotubes grown from the acetonitrile solely (Fig. 2b) evidences the high rate recombination of the nitrogen and carbon atoms. The observation that the concentration of pyridinic nitrogen decreases from the surface to depth of the nanotube, while the concentration of the graphitic nitrogen has an opposite behavior supports the catalytic thermolysis of acetonitrile and benzylamine at 800°C down to individual atoms. The atoms should move more easily through the subsurface layers and the bulk of metallic nanoparticle than a bonded combination of atoms, such as a CN pair.

A rise of the N/C ratio in the precursor vapor results in higher concentrations of N_2 trapped in the N–MWCNTs core. Since these molecules are in the nanotube cavity or between the inner layers, it is likely that they were generated as a result of nitrogen atoms diffusing through the catalyst particle. Recently, Kamberger *et al.* detected N_2 molecules in single-walled CNTs, produced from an isotope labeled acetonitrile, and explained their existence by the reaction of two C≡N radicals at or inside the catalyst particle.[48] According to NEXAFS and XPS data, this reaction is less likely to occur in N–MWCNTs, but cannot be excluded.

In summary, we illustrate the formation mechanism of N–MWCNTs and distribution of different forms of nitrogen along the nanotube layers as depicted in Figure 6a. The shape and location of catalyst nanoparticle were adopted from TEM images and are typical for N–MWCNTs (Fig. 6b). At the catalyst surface, the nitrogen-containing precursor decomposes to atoms. These atoms interact on the metallic surface producing CN and NH species or diffuse through the catalyst nanoparticle. Surface and subsurface diffusion of the CN and NH contribute in the formation of pyridinic and pyrrolic nitrogen mainly in the outer shells of N–MWCNTs. Bulk diffusion of C and N atoms results in building of the shells enriched with graphitic nitrogen and these shells are closer to the nanotube core. Because graphitic shells can preserve the tubular

shape when only restricted amount of nitrogen atoms are incorporated, the rest of the nitrogen atoms diffusing through the catalyst contribute to the formation of N_2 molecules, which is also confirmed with Mössbauer spectroscopy study of N–MWCNTs.[49] The nanotubes, produced in similar conditions as reported here, contained no α-Fe phase, due to the dissolution of nitrogen in the iron catalyst nanoparticles.

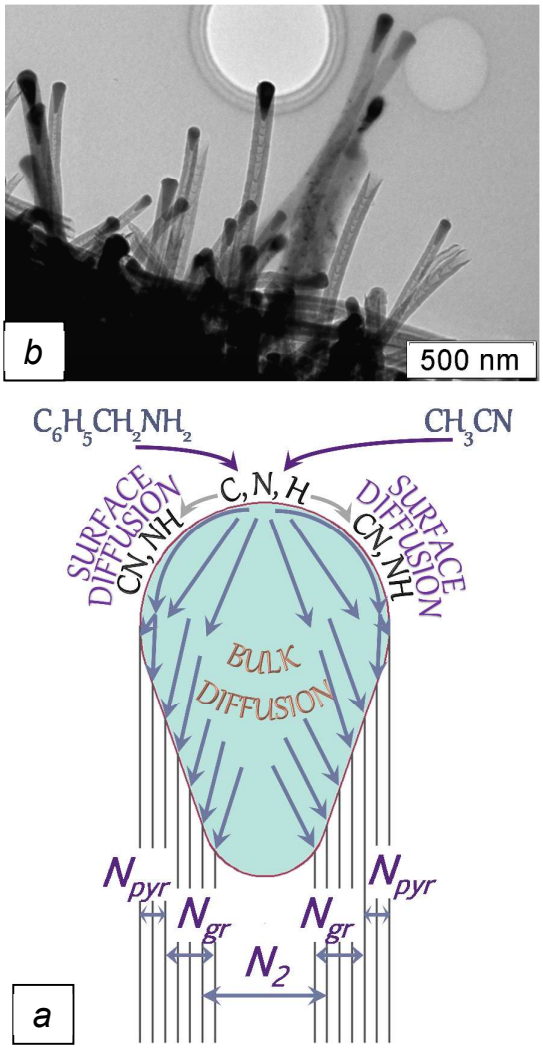

Fig. 6 Schematic diagram of the formation and preferred distribution of different forms of nitrogen (N_{pyr} – pyridinic and pyrrolic, N_{gr} – graphitic) in N–MWCNTs (a). TEM image of the tips of N–MWCNTs synthesized from acetonitrile:toluene of 50:50 (b) served as a basis for the shape and location of catalyst nanoparticle shown in (a).

5. Conclusion

Different C–N bonding environments may lead to nanotubes with significantly different properties, therefore we comparatively examined N–MWCNTs grown from molecules

incorporating significantly different bonds namely acetonitrile CH_3CN and benzylamine $C_6H_5CH_2NH_2$. We investigated multi-wall carbon nanotubes produced by aerosol assisted CCVD from pure and diluted nitrogen-containing precursors using surface sensitive XPS and bulk probing NEXAFS spectroscopy in order to study and characterize the incorporation and nature of nitrogen atoms within the graphitic network of the MWCNTs. Four chemical forms of nitrogen, namely, pyridinic, pyrrolic, and graphitic configurations and N_2 molecules were found in the N–MWCNTs independently of the feedstock composition. Analysis of the spectral data revealed no obvious effect of the nature of nitrogen-containing precursor on probability of the realization of any nitrogen form, while we found dependence on the N/C ratio in reactants. Increase of the nitrogen content in the feedstock suppresses incorporation of the pyrrolic nitrogen first and induces the N_2 formation substantially. We suggest that CN and NH species diffuse on the surface or in subsurface layers of catalyst nanoparticle, while C and N atoms diffuse in bulk. Consequently, the properties of N–MWCNTs are independent of the feedstock composition. But it is possible to tune the N incorporation with N/C ratio in precursors, hence their applicability may be extended. Therefore cheap nitrogen precursors should be used and the cost of manufacturing may be reduced. The results obtained are also important for precise control of the CNT composition through the tuning the synthesis conditions. Further experiments are envisaged to explore additional experimental parameters to control the N incorporation and reduce the cost of N–MWCNT production.

Acknowledgements

We thank A. V. Ishchenko for the TEM images. The work was supported by the Russian Foundation for Basic Research (grant 13-03-00884-a) and the bilateral Program "Russian-German Laboratory at BESSY" in part of the XPS and NEXAFS measurements. We are also grateful for the financial support received from the European Community's Seventh Framework Programme (FP7/2007–2013): the Marie Curie CONTACT Project under grant agreement no. 238363; The Royal Society, European Research Council (ERC) Starting Grant (ERC-2009-StG

240500 DEDIGROWTH; and ERC-2012-PoC 309786 DEVICE); UK Government for Engineering and Physical Sciences Research Council (EPSRC) Pathways to Impact grants.

Notes and rederences

1. C. P. Ewels and M. Glerup, *J. Nanosci. Nanotech*., 2005, **5**, 1345.
2. P. Ayala, R. Arenal, M. Rümmeli, A. Rubio and T. Pichler, *Carbon*, 2010, **48**, 575.
3. D. Jana, C.-L. Sun, L.-C. Chen and K.-H. Chen, *Progr. Mater. Sci.*, 2013, **58**, 565.
4. K.-Y. Chun, H.S. Lee and C.J. Lee, *Carbon*, 2009, **47**, 169.
5. L. G. Bulusheva, O. V. Sedelnikova and A. V. Okotrub, *Int. J. Quant. Chem.*, 2011, **111**, 2696.
6. A. Okotrub, A. Kudashov, A. Gusel'nikov and L. Bulusheva in *Phys., Chem. Appl. Nanostruct.* ed. V. E. Borisenko, S. V. Gaponenko and V. S. Gurin, Proceedings of the International Conference. Nanomeeting-2007, Minsk, Belarus, 22-25 May 2007, Review and Short Notes. pp. 585-588.
7. L. Jia, D.A. Bulusheva, O.Yu. Podyacheva, A.I. Boronin, L.S. Kibis, E.Yu. Gerasimov, S. Beloshapkin, I.A. Seryak, Z.R. Ismagilov and J.R.H. Ross, *J. Catal.*, 2013, **307**, 94.
8. X. Lepró, E. Terrés, Y. Vega-Cantú, F.J. Rodríguez-Macías, H. Muramatsu, Y. A. Kim, T. Hayahsi, M. Endo, M. Torres R., M. Terrones, *Chem. Phys. Lett.*, 2008, **463**, 124.
9. L. F. Mabena, S. S. Ray, S. D. Mhlanga and N. J. Coville, *Appl. Nanosci.*, 2011, **1**, 67.
10. Y. Zhang, C. Liu, B. Wen, X. Song and T. Li, *Mater. Lett.*, 2011, **65**, 49.
11. L. G. Bulusheva, E. O. Fedorovskaya, A. G. Kurenya and A. V. Okotrub, *Phys. Status Solidi B*, 2013, **250**, 2586.
12. L. G. Bulusheva, A. V. Okotrub, A. G. Kurenya, H. Zhang, H. Zhang, X. Chen and H. Song, *Carbon*, 2011, **49**, 4013.
13. X. Li, J. Liu, Y. Zhang, Y. Li, H. Liu, X. Meng, Y. Yang, D. Geng, D. Wang, R. Li and X. Sun, *J. Pow. Sour.*, 2012, **197**, 238.
14. S. van Dommele, A. Romero-Izquirdo, R. Brydson, K.P. de Jong and J.H. Bitter, *Carbon*, 2008, **46**, 138.
15. J. Liu, S. Webster and D.L. Carroll, *J. Phys. Chem. B*, 2005, **109**, 15769.

16. L. G. Bulusheva, A. V. Okotrub, A. G. Kudashov, E. N. Pazhetnov, A. I. Boronin and D. V. Vyalikh, *Phys. Stat. Sol. B*, 2007, **244**, 4078.

17. E. N. Nxumalo and N. J. Coville, *Materials*, 2010, **3**, 2141.

18. T. Sharifi, F. Nitze, H.R. Barzegar, C.-W. Tai, M. Mazurkeiwicz, A. Malolepszy, L. Stobinski and T. Wågberg, *Carbon*, 2012, **50**, 3535.

19. M. Scardamaglia, M. Amati, B. Llorente, P. Mudimela, J.-F. Colomer, J. Ghijsen, C. Ewels, R. Snyders, L. Gregoratti and C. Bittencourt, *Carbon*, 2014, **77**, 319.

20. T. Susi, T. Pichler and P. Ayala, *Beilstein J. Nanotech.*, 2015, **6**, 177.

21. K. Chizari, A. Vena, L. Laurentius and U. Sundararaj, *Carbon*, 2014, **68**, 369.

22. H. Liu, Y. Zhang, R. Li, X. Sun and H. Abou-Rachid, *J. Nanopart. Res.*, 2012, **14**, 1016.

23. G. Bepete, Z.N. Tetana, S. Lindner, M.R. Rümmeli, Z. Chiguvare and N.J. Coville, *Carbon*, 2013, **52**, 316.

24. H. Liu, Y. Zhang, R. Li, X. Sun, S. Désilets, H. Abou-Rachid, M. Jaidann and L.-S. Lussier, *Carbon*, 2010, **48**, 1490.

25. G. Jian, Y. Zhao, Q. Wu, L. Yang, X. Wang and Z. Hu, *J. Phys. Chem. C*, 2013, **117**, 7811.

26. E. N. Nxumalo, P. J. Letsoalo, L. M. Cele and N. J. Coville, *J. Organimet. Chem.*, 2010, **695**, 2596.

27. K. J. MacKenzie, O. M. Dunens and A. T. Harris, *Ind. Eng. Chem. Res.*, 2010, **49**, 5323.

28. S. S. Meysami, A. A. Koós, F. Dillon and N. Grobert, *Carbon*, 2013, **58**, 159.

29. V. Jourdain and C. Bichara, *Carbon*, 2013, **58**, 2.

30. T. Susi, G. Lanzani, A. G. Nasibulin, P. Ayala, T. Jiang, T. Bligaard, K. Laasonen and E. I. Kauppinen, *Phys. Chem. Chem. Phys.*, 2011, **13**, 11303.

31. S. Taubert and K. Laasonen, *J. Phys. Chem.*, 2012, **116**, 18538.

32. A. A. Koós, M. Dowling, K. Jurkschat, A. Crossley and N. Grobert, *Carbon*, 2009, **47**, 30.

33. A. G. Kudashov, A. G. Kurenya, A. V. Okotrub, A. V. Gusel'nikov, V. S. Danilovich and L. G. Bulusheva, *Techn. Phys.*, 2007, **52**, 1627.

34. R. J. Nicholls, Z. Aslam, M. C. Sarahan, A. M. Sanchez, F. Dillon, A. A. Koós, P. D. Nellist and N. Grobert, *Phys. Chem. Chem. Phys.*, 2015, **17**, 2137.

35. J. W. Jang, C. E. Lee, S. C. Lyu, T. J. Lee and C. J. Lee, *Appl. Phys. Lett.*, 2004, **84**, 2877.

36. M. P. Seah and W. A. Dench, *Surf. Interface Anal.*, 1979, **1**, 2.

37. S. Doniach and M. Sunjic, *J. Phys. C: Solid State Phys.*, 1970, **3**, 285.

38. J.-P. Savy, D. de Caro, C. Faulmann, L. Valade, M. Almeida, T. Koike, H. Fujiwara, T. Sugimoto, J. Fraxedas, T. Ondarçuhu and C. Pasquier, *New J. Chem.*, 2007, **31**, 519.

39. C. Puglia, P. Bennich, J. Hasselström, C. Ribbing, P.A. Brühwiler, A. Nilson, Z.Y. Li, and N. Mårtensson, *Surf. Sci.*, 1998, **414**, 118.

40. J. Zhou, J. Wang, H. Liu, M. N. Banis, X. Sun, and T.-K. Sham, *J. Phys. Chem. Lett.*, 2010, **1**, 1709.

41. H. C. Choi, J. Park and B. Kim, *J. Phys. Chem. B*, 2005, **109**, 4333.

42. J. H. Yang, D. H. Lee, M. H. Yum, Y. S. Shin, E. J. Kim, C.-Y. Park, M. H. Kwon, C. W. Yang, J.-B. Yoo, H.-J. Song, H.-J. Shin, Y.-W. Jin and J.-M. Kim, *Carbon*, 2006, **44**, 2219.

43. A. V. Okotrub, L. G. Bulusheva, A. G. Kudashov, V. V. Belavin, D. V. Vyalikh and S. L. Molodtsov, *Appl. Phys. A*, 2009, **94**, 437.

44. A.P. Hitchcock and C.E. Brion, *Chem. Phys.*, 1979, **37**, 319.

45. A. Majumdar, S.C. Das, T. Shripathi, J. Heinicke and R. Hipper, *Surf. Sci.*, 2013, **609**, 53.

46. L. G. Bulusheva, A. V. Okotrub, A. G. Kudashov, Yu. V. Shubin, E. V. Shlyakhova, N. F. Yudanov, E. M. Pazhetnov, A. I. Boronin and D. V. Vyalikh, *Carbon*, 2008, **46**, 864.

47. S. Y. Kim, J. Lee, C. W. Na, J. Park, K. Seo and B. Kim, *Chem. Phys. Lett.*, 2005, **413**, 3000.

48. C. Kramberger, T. Thurakitseree, E. Einarsson, A. Takashima, T. Kinoshita, T. Muro and S. Maruyama, *Nanoscale*, 2014, **6**, 1525.

49. I. S. Lyubutin, O. A. Anosova, K. V. Frolov, S. N. Sulyanov, A. V. Okotrub, A. G. Kudashov and L. G. Bulusheva, *Carbon*, 2012, **50**, 2628.